SUPPLEMENTARY DATA

Supplemental Materials

MRI data acquisition

Imaging data were collected using a SIEMENS TRIO 3-Tesla MRI system including DTI data and T1-weighted images scans. Participants were in a supine position with their head snugly fixed by straps and foam pads to minimize head movement. Diffusion-weighted imaging was performed using a single-shot, twice-refocused, diffusion-weighted echo planar sequence aligned along the anterior-posterior commissural plane. The DTI was acquired according to the following parameters: field of view = 256×256 mm^2, repetition time/echo time = 9500/92 ms, matrix = 128×128, slice thickness = 2 mm, and 70 continuous axial slices with no gap. Diffusion sensitizing gradients were applied along a 30 nonlinear direction (b = 1000 s/mm^2) and in one direction for non-diffusion weighting (b = 0 s/mm^2). T1-weighted images were also acquired to measure the cerebral gray matter density. T1-weighted, sagittal 3D magnetization prepared rapid gradient echo (MP-RAGE) sequences were collected using an echo-planar imaging sequence that consisted of a 176 sagittal slices, repetition time/echo time = 1900/3.44 ms, slice thickness = 1 mm, flip angle = 9°, inversion time = 900 ms, field of view (FOV) = 256×256 mm^2, and acquisition matrix = 256×256.

DTI data preprocessing and analysis

FMRIB's Diffusion Toolbox (FDT, v3.0) in FMRIB Software Library (FSL, v5.0.10) were used for image preprocessing. First, eddy current distortions and motion artifacts were corrected by applying affine alignment of each diffusion-weighted image to the b = 0 image. Then, the first volume of the diffusion data with no diffusion weighting (i.e., b=0 image) was used to create a brain mask by running the Brain Extraction Tool. Finally, we fit a diffusion tensor model at each voxel using DTIFIT. The output of DTIFIT yielded voxel-wise maps of fractional anisotropy and axial diffusivity. The fractional anisotropy index of DTI is the most sensitive neuroimaging measures of the degeneration observed in T2DM patients, and it describes overall white matter health, maturation, and organization (1). Another index, axial diffusivity, reflects axon integrity and can be useful in understanding the underlying physiology (2).

Voxel-wise analyses of the fractional anisotropy and axial diffusivity images were carried out using Tract-Based Spatial Statistics (TBSS) in FSL. First, each participant's fractional anisotropy image was aligned to the 1×1×1 mm FMRIB58_FA standard space using the nonlinear registration (3). Second, all subjects were affine-aligned into a 1×1×1 mm MNI152 space. Third, the mean of all fractional anisotropy images was created and fed into the fractional anisotropy skeletonization program to create a mean fractional anisotropy skeleton (threshold of 0.2) from all subjects included in this study. Then, the 4D all fractional anisotropy image (containing all aligned fractional anisotropy data from all subjects) was projected onto the mean fractional anisotropy skeleton, and this approach resulted in a 4D image file containing the (projected) skeletonized fractional anisotropy data. Finally, we applied TBSS to axial diffusion using the fractional anisotropy images to achieve the nonlinear registration and skeletonization stages, which resulted in the 4D projected axial diffusion data. Those projected data files were fed into voxel-wise statistics.

Voxel-wise statistical analyses were carried out using nonparametric permutation-based inference tool ("randomize", part of FSL) with the general linear model (GLM) as statistical modeling. First, pair-wise group comparisons based on voxel were performed using GLM for T2DM-aMCI versus HC, T2DM-aMCI versus T2DM-NC, and T2DM-NC versus HC. The fractional anisotropy or axial diffusion at each voxel were modeled as a linear combination of predictors (three grouping variables) and covariates (sex, age, education, hypertension, hyperlipidemia and cerebrovascular disease) stored in the columns of a "design matrix". For subsequent analyses, we calculated white matter volumes in regions with between-group differences, fractional anisotropy and axial diffusivity at voxels within significant intergroup different tracts in combining the T2DM-aMCI and T2DM-NC patients. White matter tracts were identified using the JHU_ICBM_tracts_maxprob_thr25 atlas (4). Second, a voxel-wise linear relationship was determined using GLM in all T2DM (T2DM-aMCI combined with T2DM-NC). The

fractional anisotropy or axial diffusion at each voxel in significant intergroup different tracts is modeled as a linear combination of cognitive scores with significant intergroup difference domains and covariates. The significance threshold for between-group differences and linear relationships were set at $p < 0.05$ (5000 permutations, familywise error (FWE) correction for multiple comparisons correction) using the threshold-free cluster enhancement (TFCE). Next, we extract the mean value of axial diffusivity on significantly related fibers for subsequent analyses. Fractional anisotropy of significant intergroup different tracts didn't showed any significant relationships with cognitive measures.

T1 MRI data processing and analysis

T1-weighted images were analyzed with the FSL voxel-based morphometry (FSLVBM) pipeline (5). First, brain extraction was run on the structural images. Second, all brain-extracted images were segmented into gray matter, white matter and cerebrospinal fluid. Third, the symmetric, study-specific nonlinear gray matter template in a standard space was created from the segmented (gray matter) images with an equal number of T2DM-aMCI patients and T2DM-NC patients who were selected randomly. To achieve this, these selected gray matter images were affine-registered to a gray matter ICBM-152 template, concatenated and then averaged. This averaged image was then flipped along the x-axis and the two mirror images, then re-averaged to obtain a symmetric affine gray matter template. And selected gray matter images were reregistered to this specific affine gray matter template using nonlinear registration, then were concatenated into a 4D image, averaged, and flipped along the x-axis. Both mirror images were then averaged to create the final template. Finally, modulation was implemented to the contraction/enlargement due to the nonlinear component of the transformation in which each voxel of each registered gray matter image is multiplied by the Jacobian of the warp field. All the modulated registered gray matter images were concatenated into a 4D image, and the file was fed into voxel-vise statistics.

Next, a voxel-wise linear relationship was determined with GLM in all T2DM using a randomize tool to evaluate whether cognitive impairment-related white matter microstructural damage was associated with the degeneration of cortex connected to the affected white matter tract. The gray matter density in regions of interests (ROIs) at each voxel was modeled as a linear regression of diffusion metrics in cognitive impairment-related white matter tracts and covariates (sex, age, education, hypertension, hyperlipidemia and cerebrovascular disease). The significance threshold for a linear relationship was set at $p < 0.05$ (5000 permutations, FWE-correction for multiple comparisons). In this study, the gray matter ROIs were the lingual and frontal middle orbital (Frontal_Mid_Orb) with anatomic connections to IFOF as well as the temporal inferior (Temporal_Inf) and occipital middle (Occipital_Mid) with anatomic connections to ILF (6).

SUPPLEMENTARY DATA

Supplementary Figure S1. The mean score of neuropsychological tests in T2DM-aMCI, T2DM-NC and HC groups. *p < 0.05, **p < 0.01, ***p < 0.001 after Bonferroni correction.

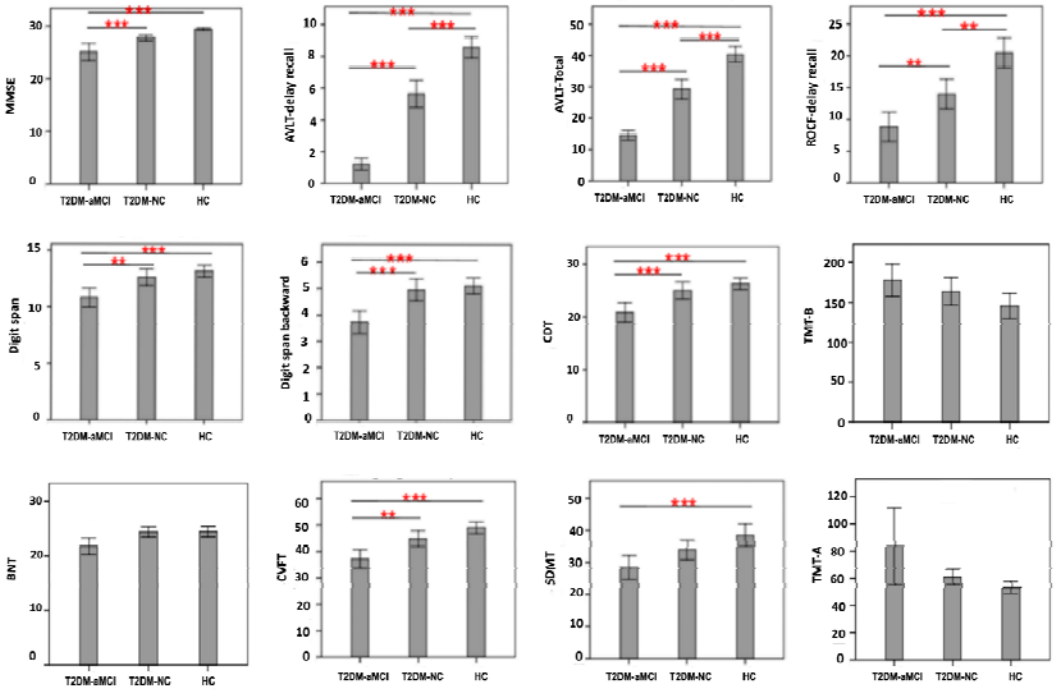

SUPPLEMENTARY DATA

Supplementary Table S1. The below table present the normalized cognitive scores as well in z-values and the percentage of patients with a score below 1.5SD (across all participants).

group	T2DM-aMCI	T2DM-NC	HC	Patients with a score below 1.5SD (N, %)	
				T2DM-aMCI	T2DM-NC
General Mental status					
MMSE	-0.72 ± 1.45	0.08 ± 0.46	0.57 ± 0.22	7 (19.44%)	0
Episodic Memory					
AVLT-delay recall (N5)	-1.14 ± 0.3	0.08 ± 0.73	0.89 ± 0.57	0	0
AVLT-Total (N1-N5)	-1.1 ± 0.34	0.04 ± 0.74	0.9 ± 0.61	4 (11.11%)	4 (10%)
ROCF-delay recall	-0.71 ± 0.78	-0.1 ± 0.85	0.68 ± 0.87	5 (13.89%)	3 (7.5%)
Working memory					
Digit Span	-0.65 ± 1.03	0.14 ± 0.99	0.38 ± 0.7	8 (22.22%)	4 (10%)
Digit Span Backward	-0.72 ± 0.93	0.23 ± 0.99	0.35 ± 0.74	14 (38.89%)	4 (10%)
Spatial processing					
ROCF-Copy	-0.34 ± 1.36	0.12 ± 0.63	0.17 ± 0.89	3 (8.33%)	1 (2.5%)
CDT	-0.65 ± 1.07	0.16 ± 0.96	0.41 ± 0.65	7 (19.45)	3 (7.5%)
Executive function					
SCWT-C-B	0.08 ± 1.06	0.04 ± 1.02	-0.16 ± 0.96	2 (5.56%)	0
TMT-B	0.21 ± 1.16	0.06 ± 1.02	-0.28 ± 0.93	1 (2.78%)	1 (2.5%)
Language ability					
BNT	-0.51 ± 1.22	0.22 ± 0.79	0.23 ± 0.81	12 (33.33%)	3 (7.5%)
CVFT	-0.69 ± 1	0.08 ± 0.93	0.5 ± 0.71	14 (38.89%)	4 (10%)
Attention					
SDMT	-0.7 ± 1.09	-0.02 ± 0.88	0.41 ± 1.01	5 (13.89%)	0
TMT-A	0.37 ± 1.75	-0.08 ± 0.4	-0.25 ± 0.31	0	0

Note: Values are the mean ± standard deviation. MMSE: Mini-Mental State Examination, AVLT: Auditory Verbal Learning Test, ROCF: Rey-Osterrieth Complex Figure, CDT: Clock Drawing Test, SCWT: Stroop Color and Word Test, TMT: Trail Making Test, BNT: Boston Naming Test, CVFT: Category Verbal Fluency Test, SDMT: Symbol Digit Modalities Test.

SUPPLEMENTARY DATA

Supplementary Table S2. White matter integrity differences between T2DM-aMCI and HC patients.

Tracts		T2DM-aMCI vs HC Volumes (mm^3)
1	ATR.L	289
2	ATR.R	144
3	CST.L	68
4	CST.R	105
5	CG.L	31
6	CG.R	11
7	CH.L	0
8	CH.R	3
9	Fmaj	252
10	Fmin	488
11	IFOF.L	236
12	IFOF.R	428
13	ILF.L	61
14	ILF.R	158
15	SLF.L	55
16	SLF.T	230
17	UF.L	111
18	UF.R	58
19	SLF-temp.L	19
20	SLF-temp.R	77

Results showed radial diffusivity increased of multiple fibers across the whole brain between T2DM-aMCI and HC group.

1. Basser, P.J. and C. Pierpaoli, *Microstructural and physiological features of tissues elucidated by quantitative-diffusion-tensor MRI.* J Magn Reson B, 1996. **111**(3): p. 209-219.
2. Budde, M.D., et al., *Toward accurate diagnosis of white matter pathology using diffusion tensor imaging.* Magnetic Resonance in Medicine, 2007. **57**(4): p. 688-695.
3. Ashburner, J. and K. Friston, *Non-linear Registration*. 2007.
4. Mori, S., et al., *Stereotaxic white matter atlas based on diffusion tensor imaging in an ICBM template.* Neuroimage, 2008. **40**(2): p. 570-582.
5. Smith, S.M., et al., *Advances in functional and structural MR image analysis and implementation as FSL*. Neuroimage, 2004. **23**: p. S208-S219.
6. Gong, G.L., et al., *Mapping Anatomical Connectivity Patterns of Human Cerebral Cortex Using In Vivo Diffusion Tensor Imaging Tractography.* Cerebral Cortex, 2009. **19**(3): p. 524-536.